J|A|C|S
ARTICLES
Published on Web 05/17/2005

Helical Structures of *N*-Alkylated Poly(*p*-benzamide)s

Aya Tanatani,[†,‡] Akihiro Yokoyama,[§] Isao Azumaya,[||] Yoshinori Takakura,[§] Chikashi Mitsui,[§] Motoo Shiro,[⊥] Masanobu Uchiyama,[†,@] Atsuya Muranaka,[#] Nagao Kobayashi,*[,#] and Tsutomu Yokozawa*[,†,§]

Contribution from the Synthesis and Control, PRESTO, Japan Science and Technology Agency (JST), Japan, Department of Applied Chemistry, Kanagawa University, Rokkakubashi, Kanagawa-ku, Yokohama 221-8686, Japan, Faculty of Pharmaceutical Sciences at Kagawa Campus, Tokushima Bunri University, 1314-1 Shido, Sanuki, Kagawa 769-2193, Japan, Rigaku Corporation, X-ray Research Laboratory, Matsubaracho 3-9-12, Akishima, Tokyo 196-8666, Japan, Graduate School of Pharmaceutical Sciences, The University of Tokyo, 7-3-1 Hongo, Bunkyo-ku, Tokyo 113-0033, Japan, and Department of Chemistry, Graduate School of Science, Tohoku University, Sendai 980-8578, Japan

Received July 26, 2004; E-mail: yokozt01@kanagawa-u.ac.jp; nagaok@mail.tains.tohoku.ac.jp

Abstract: Poly(*p*-benzamide)s **1** bearing a chiral side chain on the nitrogen atom were synthesized by chain-growth polycondensation methodology. The polyamides exhibited well-defined molecular weights with narrow polydispersities. Solutions of the polyamides in several organic solvents (CH_3CN, $CHCl_3$, and CH_3OH) showed dispersion type CD signals characteristic of coupled-oscillator and much larger as compared with the corresponding monomer. The CD signals were dependent on the temperature and molecular weight of the polyamides but independent of the solvent, as far as examined. An exciton model analysis of the absorption and CD spectra provided a clear-cut picture for the secondary structure of these polyamides in solution that the *N*-alkylated poly(*p*-benzamide)s possess a right-handed helical conformation ((*P*)-helix). In the solid states, the results of X-ray crystallographic analysis of 4-(methylamino)benzoic acid oligomers substantiated that they have a helical conformation with three monomer units per turn.

Introduction

The helix is nature's most attractive and important conformational motif, as seen in the structure and function of DNA and proteins.[1] Great efforts have been made to understand the properties of helical structure and to construct helical polymers[2] and oligomers[3] possessing useful functions, such as molecular recognition of chiral guests and asymmetric catalytic ability in organic synthesis. In contrast to stable helical polymers with a rigid backbone, polyisocyanates,[4] polysilanes,[5] and polyacetylenes[6] are helical polymers consisting of a stiff backbone, within which helix−helix or helix−coil interconversion readily occurs due to the small energetic barriers to helical reversal. These helical polymers are classified as dynamic helical polymers and are characterized by a dependence of the helical conformation in solution upon polymer chain length, temperature,[7] and so forth.

Aromatic polyamides composed of *N*-unsubstituted amide bonds, such as poly(*p*-phenylene terephthalamide) and poly(*p*-benzamide), possess extended rodlike structures.[8] The amide linkages of these polymers are in trans conformation[9] and form hydrogen bonds between polymer chains to give a sheet structure. If the nitrogen of the amide bonds is alkylated, the polymers are thought to take coiled structures,[10] although no detailed investigation to elucidate their structures has been reported. On the other hand, the conformation of *N*-alkylated

[†] PRESTO, JST.
[‡] Current address: Institute of Molecular and Cellular Biosciences, The University of Tokyo, Tokyo, Japan.
[§] Kanagawa University.
[||] Tokushima Bunri University.
[⊥] Rigaku Corporation.
[@] The University of Tokyo.
[#] Tohoku University.

(1) (a) Watson, J. D.; Crick, F. H. C. *Nature* **1953**, *171*, 737−738. (b) Branden, C.; Tooze, J. *Introduction to Protein Structure*; Garland: New York, 1991.
(2) (a) Nakano, T.; Okamoto, Y. *Chem. Rev.* **2001**, *101*, 4013−4038. (b) Cornelissen, J. J. L. M.; Rowan, A. E.; Nolte, R. J. M.; Sommerdiik, N. A. J. M. *Chem. Rev.* **2001**, *101*, 4039−4070.
(3) (a) Gellman, S. H. *Acc. Chem. Res.* **1998**, *31*, 173−180. (b) Rowan, A. E.; Nolte, R. J. M. *Angew. Chem., Int. Ed. Engl.* **1998**, *37*, 63−68. (c) Katz, T. J. *Angew. Chem., Int. Ed.* **2000**, *39*, 1921−1923. (d) Hill, D. J.; Mio, M. J.; Prince, R. B.; Hughes, T. S.; Moore, J. S. *Chem. Rev.* **2001**, *101*, 3893−4011. (e) Schmuck, C. *Angew. Chem., Int. Ed.* **2003**, *42*, 2448−2452.
(4) (a) Green, M. M.; Peterson, N. C.; Sato, T.; Teramoto, A.; Cook, R.; Lifson, S. *Science* **1995**, *268*, 1860−1866. (b) Okamoto, Y.; Matsuda, M.; Nakano, T.; Yashima, E. *J. Polym. Sci., Part A: Polym. Chem.* **1994**, *32*, 309−315. (c) Mruk, R.; Zentel, R. *Macromolecules* **2002**, *35*, 185−192.
(5) Fujiki, M. *J. Am. Chem. Soc.* **2000**, *122*, 3336−3343.
(6) (a) Ciardelli, F.; Lanzillo, S.; Pieroni, O. *Macromolecules* **1974**, *7*, 174−179. (b) Moore, J. S.; Gorman, C. B.; Grubbs, R. H. *J. Am. Chem. Soc.* **1991**, *113*, 1704−1712. (c) Yashima, E.; Huang, S.; Matsushima, T.; Okamoto, Y. *Macromolecules* **1995**, *28*, 4184−4193. (d) Nomura, R.; Fukushima, Y.; Nakako, H.; Masuda, T. *J. Am. Chem. Soc.* **2000**, *122*, 8830−8836.
(7) (a) Nelson, J. C.; Saven, J. G.; Moore, J. S.; Wolynes, P. G. *Science* **1997**, *277*, 1793−1796. (b) Takata, T.; Furusho, Y.; Murakawa, K.; Endo, T.; Matsuoka, H.; Hirasa, T.; Matsuo, J.; Sisido, M. *J. Am. Chem. Soc.* **1998**, *120*, 4530−4531.
(8) (a) Northolt, M. G.; van Aartsen, J. J. *J. Polym. Sci., Polym. Lett. Ed.* **1973**, *11*, 333−337. (b) Northolt, M. G. *Eur. Polym. J.* **1974**, *10*, 799−804. (c) Tashiro, K.; Kobayashi, M.; Tadokoro, H. *Macromolecules* **1977**, *10*, 413−420.
(9) In this paper, the terms cis and trans amide conformation are used to show the relative positions of aromatic groups connected to the amide group.

aromatic amides of low molecular weight has been investigated in detail, and it was shown that *N*-alkylated aromatic amides favor the cis conformation in the crystal and in solution.[11] Further, X-ray analysis of *N*,*N*′-dimethyl-*N*,*N*′-diphenylbenzenedicarboxamides demonstrated that, when three benzene units are connected by two *N*-alkylated amide bonds, the amide bonds adopt the cis conformation, and the three benzene units are not coplanar.[12] In this case, the terminal benzene rings can be arranged in two ways: on opposite sides (anti conformation) or on the same side (syn conformation) of the central benzene ring.

These results, as well as the finding that the condensation of 4-(methylamino)benzoic acid gave exclusively the cyclic trimer,[13] led us to postulate that *N*-alkylated poly(*p*-benzamide)s may form a helical conformation in solution, despite their high flexibility as compared to the known helical polymers and lack of apparent force to fix the backbone. Further, we have developed a chain-growth polycondensation methodology to synthesize *N*-alkylated poly(*p*-benzamide)s with well-controlled molecular weight and narrow polydispersity ($M_w/M_n \leq 1.1$).[14] Because the method provides *N*-alkylated poly(*p*-benzamide)s having desired length and narrow polydispersity without difficulty or cumbersome fractionation, it will be helpful to gain an understanding of the chain length-dependent chiroptical properties of this important class of aromatic polyamides (aramides). In this paper, we show that *N*-alkylated poly(*p*-benzamide)s **1** bearing a chiral side chain on the nitrogen atom take a right-handed helical structure in solution.[15] The temperature-[16] and chain length-dependent[17] circular dichroism (CD) signals indicate that the polyamides have dynamic helical properties. The helical structure of the *N*-alkylated aromatic polyamides is clearly and unambiguously supported by the exciton analysis of both electronic absorption and CD spectra. The X-ray crystallographic analysis of the oligomers of 4-(methylamino)benzoic acid demonstrates that they have a helical conformation with three monomer units per turn in the crystal.

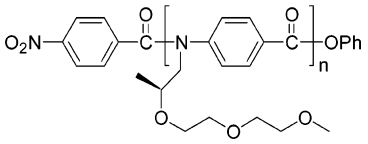

Polyamide **1**

Results and Discussion

1. Synthesis of Polyamides. We designed poly(*p*-benzamide)s **1** possessing an *N*-(*S*)-2-(methoxyethoxyethoxy)propyl group as a chiral side chain because poly(*p*-benzamide)s having a tri(ethylene glycol) monomethyl ether unit on the nitrogen atom show higher solubility than those with an octyl or dodecyl unit.[18] To synthesize the polyamides with our chain-growth polycondensation methodology, we first prepared the monomer **2** as shown in Scheme 1. Introduction of the chiral side chain into the 4-aminobenzoate unit was achieved by Fukuyama's method[19] using sulfonamide and chiral alcohol. Thus, phenyl 4-aminobenzoate **3**[14b] was converted to sulfonamide **4** by treatment with 2-nitrobenzenesulfonyl chloride. Alkylation of **4** was carried out under the Mitsunobu conditions with **5,** which was prepared as described in the literature.[20] Removal of the 2-nitrobenzenesulfonyl group from **6** was performed by treatment with PhSH and Cs_2CO_3 to give the monomer **2** in high yield.

Scheme 1. Synthesis of Monomer **2**

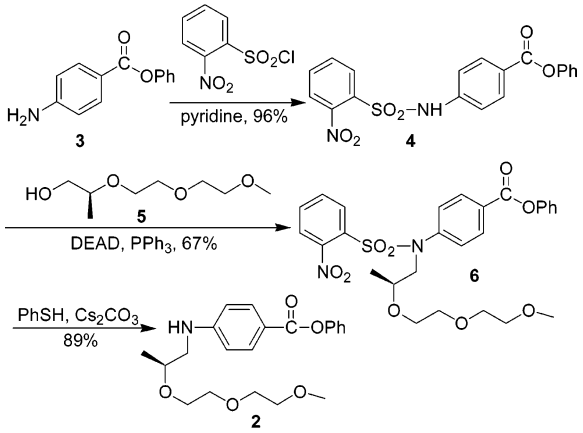

Scheme 2. Chain-Growth Polycondensation for Polyamides **1**

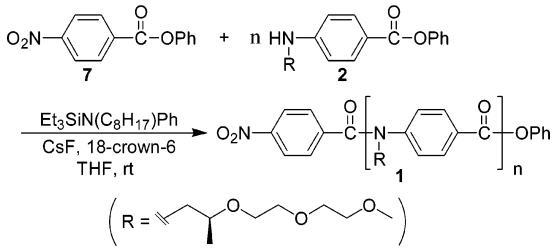

Chain-growth polycondensation of **2** was carried out in the presence of the initiator **7** using a combination of *N*-octyl-*N*-triethylsilylaniline, CsF, and 18-crown-6 as a base[14a] (Scheme 2). Polyamides **1a**−**f** with varying lengths (M_n = 1700−14 300) and narrow polydispersities (M_w/M_n = 1.05−1.17) were obtained by changing the feed ratio of **7** to **2** (Table 1).

2. UV and CD Investigations of Chiral Polyamides. The polyamide **1f** showed broad electronic absorption in the 240−

(10) (a) Preston, J.; Krigbaum, W. R.; Asrar, J. In *Cyclopolymerization and Polymer with Chain-Ring Structures*; Butler, G. B., Kresta, J. E., Eds.; ACS Symposium Series 195; American Chemical Society: Washington, DC, 1981; pp 351−362. (b) Burch, R. R.; Manring, L. E. *Macromolecules* **1991**, *24*, 1731−1735.

(11) (a) Itai, A.; Toriumi, Y.; Tomioka, N.; Kagechika, H.; Azumaya, I.; Shudo, K. *Tetrahedron Lett.* **1989**, *30*, 6177−6180. (b) Nishimura, T.; Maeda, K.; Yashima, E. *Chirality* **2004**, *16*, S12−S22.

(12) (a) Yamaguchi, K.; Matsumura, G.; Kagechika, H.; Azumaya, I.; Ito, Y.; Itai, A.; Shudo, K. *J. Am. Chem. Soc.* **1991**, *113*, 5474−5475. (b) Azumaya, I.; Kagechika, H.; Yamaguchi, K.; Shudo, K. *Tetrahedron* **1995**, *51*, 5277−5290.

(13) (a) Azumaya, I.; Okamoto, T.; Imabeppu, F.; Takayanagi, H. *Tetrahedron* **2003**, *59*, 2325−2331. (b) Azumaya, I.; Okamoto, T.; Imabeppu, F.; Takayanagi, H. *Heterocycles* **2003**, *60*, 1419−1424.

(14) (a) Yokozawa, T.; Asai, T.; Sugi, R.; Ishigooka, S.; Hiraoka, S. *J. Am. Chem. Soc.* **2000**, *122*, 8313−8314. (b) Yokozawa, T.; Ogawa, M.; Sekino, A.; Sugi, R.; Yokoyama, A. *J. Am. Chem. Soc.* **2002**, *124*, 15158−15159. (c) Yokozawa, T.; Yokoyama, A. *Polym. J.* **2004**, *36*, 65−83.

(15) Helical structures of aromatic polyamides without *N*-substituents. See: (a) Kondo, F.; Kakimi, S.; Kimura, H.; Takeishi, M. *Polym. Int.* **1998**, *46*, 339−344. (b) Agata, Y.; Kobayashi, M.; Kimura, H.; Takeishi, M. *Polymer* **2002**, *43*, 4829−4833.

(16) (a) Shinohara, K.; Yasuda, S.; Kato, G.; Fujita, M.; Shigekawa, H. *J. Am. Chem. Soc.* **2001**, *123*, 3619−3620. (b) Morino, K.; Maeda, K.; Okamoto, Y.; Yashima, E.; Sato, T. *Chem.*− *Eur. J.* **2002**, *8*, 5112−5120. (c) Tabei, J.; Nomura, R.; Masuda, T. *Macromolecules* **2003**, *36*, 573−577.

(17) (a) Gu, H.; Nakamura, Y.; Sato, T.; Teramoto, A.; Green, M. M.; Andreola, C.; Peterson, N. C.; Lifson, S. *Macromolecules* **1995**, *28*, 1016−1024. (b) Takei, F.; Yanai, K.; Onitsuka, K.; Takahashi, S. *Chem.*−*Eur. J.* **2000**, *6*, 983−993.

(18) Unpublished results.

(19) (a) Fukuyama, T.; Jow, C-.K.; Cheung, M. *Tetrahedron Lett.* **1995**, *36*, 6373−6374. (b) Fukuyama, T.; Cheung, M.; Jow, C.-K.; Hidai, Y.; Kan, T. *Tetrahedron Lett.* **1997**, *38*, 5831−5834.

(20) Prince, R. B.; Brunsveld, L.; Meijer, E. W.; Moore, J. S. *Angew. Chem., Int. Ed.* **2000**, *39*, 228−230.

Table 1. Molecular Weights and Polydispersities of Polyamides **1**

polymer	M_n[a]	M_w/M_n
1a	1700[b]	1.17
1b	3600	1.08
1c	5200[b]	1.06
1d	6900	1.05
1e	8000	1.05
1f	14300	1.08

[a] Measured by MALLS. [b] Calculated values obtained from the M_n(NMR) − M_n(MALLS) correlation line by using the M_n(NMR) values.

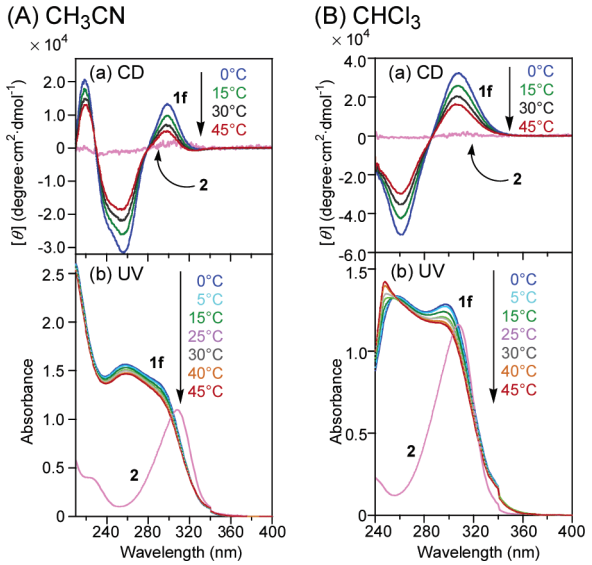

Figure 1. (a) CD and (b) UV spectra of polyamide **1f** in (A) CH_3CN and (B) $CHCl_3$ at 0 °C (blue line), 15 °C (green line), 30 °C (gray line), and 45 °C (red line) and monomer **2** at 15 °C (pink line). Concentration: [**1f**] = 60 mg/L in CH_3CN and 47 mg/L in $CHCl_3$ and [**2**] = 13 mg/L in CH_3CN and 16 mg/L in $CHCl_3$.

360 nm region, which consisted apparently of a peak at ca. 260−280 nm and a shoulder at ca. 300 nm in acetonitrile (CH_3CN), chloroform ($CHCl_3$) (Figure 1), and methanol (CH_3OH) (Figure S2 in Supporting Information). In the CD spectra, an intense (ca. 20 000 < [θ] < 50 000 at 0 °C) plus-to-minus pattern was detected in the same wavelength region, viewing from longer wavelength, and the positions of the peak and trough roughly corresponded to the two absorption peaks. Monomeric chromophore **2** showed much weaker (ca. [θ] < 1000) integral type CD signals that were similar in shape to absorption spectra aside from its sign[21] so that the intense dispersion type CD spectra are not due to the intrinsic chirality of the monomer units but to an excess of a single-handed screw-sense structure of **1**.[22] A similar CD pattern in the three solvents suggests that there is no significant influence of the solvent polarity on the conformation of the polyamides **1**. CD signals of polyamides **1** were highly temperature dependent, decreasing with increasing temperature. This observation suggests that polyamides **1** possess a flexible helical structure.

Polyamides **1** with various molecular weights exhibited similarly shaped CD spectra, but the CD intensity showed a remarkable molecular weight dependence at fixed temperatures in the range of 0−45 °C and in all solvents examined. The

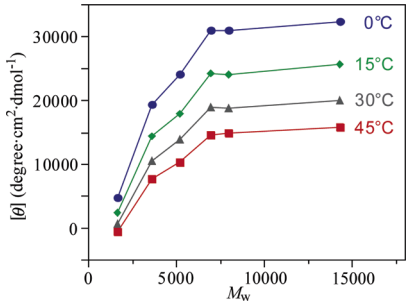

Figure 2. Dependence of CD spectra (308 nm) on molecular weight of polyamides **1** measured in $CHCl_3$ at 0 °C (blue line), 15 °C (green line), 30 °C (gray line), and 45 °C (red line). The concentration of each polymer solution was adjusted so that the absorbance at 300 nm was 1 ([**1a**−**f**] = 47−57 mg/L).

results in $CHCl_3$ are illustrated in Figure 2. Some of the salient features of this molecular weight dependence are that the CD intensity increases rapidly with increasing molecular weight when the molecular weight is small but reaches saturation when it is large. This kind of molecular weight dependence of the CD spectra is one of the criteria for judging the helical nature of the polymer, as pointed out by Green et al.[17a]

Polyamides **8**, prepared from phenyl (*R*)-(3,7-dimethyloctylamino)benzoate (**9**) as a monomer instead of **2**, did not show any significant Cotton effect at any chain length (for details of the experiments, see Supporting Information). Considering the solvent independence of the induced Cotton effect of **1**, the lack of CD spectra is not due to the hydrophobic side chain of **8** but might be due to the fact that the chiral carbon is placed one methylene unit further away from the amide backbone as compared to that of **1** and thereby has a diminished directing influence on the helicity of the polymer chain.[23]

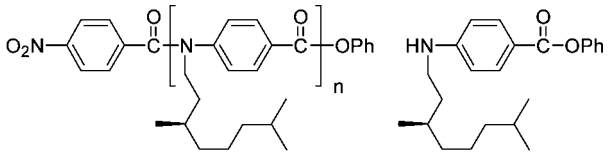

Polyamide **8** **9**

3. X-ray Crystallographic Analysis of Oligoamides. The helical structure of *N*-alkylated aromatic polyamides was further confirmed by X-ray crystallographic analysis of phenyl esters of the trimer (**10**), tetramer (**11**), and pentamer (**12**) of 4-(methylamino)benzoic acid, as well as the *N*-Cbz (Cbz: benzyloxycarbonyl) and carboxylic acid-terminated tetramer (**13**), as model compounds of the polyamides. The oligoamides **10**−**13** were synthesized by the sequential and stepwise deprotection−condensation procedure.[24] The crystallographic data are summarized in Table 2.[25]

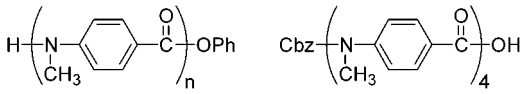

10 (n = 3), **11** (n = 4), **12** (n = 5) **13**

(21) (a) Schipper, P. E. *J. Am. Chem. Soc.* **1979**, *101*, 6826−6829. (b) Kobayashi, N.; Higashi, R.; Titeca, B. C.; Lamote, F.; Ceulemans, A. *J. Am. Chem. Soc.* **1999**, *121*, 12018−12028.
(22) Berova, N.; Nakanishi, K.; Woody, R. W. *Circular Dichroism: Principles and Applications*, 2nd ed.; Wiley-VCH: New York, 2000.
(23) Nakako, H.; Mayahara, Y.; Nomura, R.; Tabata, M.; Masuda, T. *Macromolecules* **2000**, *33*, 3978−3982.
(24) See Supporting Information for details.
(25) The space groups to which crystals **10**−**13** belong are all achiral. Therefore, a unit cell of each crystal has equal numbers of the two enantiomers (right turn and left turn) of the helices.

Table 2. Crystallographic Data

	10	11	12	13
recryst solvents	toluene	CCl_4	ethyl acetate	toluene
formula	$C_{30}H_{27}N_3O_4$	$C_{38}H_{34}N_4O_5{\cdot}2(CCl_4)$	$C_{46}H_{41}N_5O_6{\cdot}C_4H_8O_2$[a]	$C_{40}H_{36}N_4O_7{\cdot}H_2O$
formula wt	493.56	934.36	847.97	702.76
crystal system	monoclinic	monoclinic	triclinic	triclinic
a (Å)	9.921(3)	14.883(6)	11.819(2)	10.704(3)
b (Å)	18.683(3)	13.509(4)	13.490(2)	11.993(3)
c (Å)	14.218(3)	20.809(9)	15.6589(9)	13.714(3)
α (deg)			106.26(1)	87.72(2)
β (deg)	101.40(2)	92.07(4)	106.353(10)	87.36(2)
γ (deg)			100.402(5)	85.13(2)
V (Å^3)	2583.3(10)	4180(2)	2206.7(5)	1751.2(8)
space group	$P2_1/n$ (#14)	$P2_1/c$ (#14)	$P\bar{1}$ (#2)	$P\bar{1}$ (#2)
Z value	4	4	2	2
T (K)	296	93	113	93
μ (cm^{-1})	6.90 (Cu K$_\alpha$)	5.87 (Mo K$_\alpha$)	0.87 (Mo K$_\alpha$)	0.94 (Mo K$_\alpha$)
$2\theta_{max}$ (deg)	145.3	60.1	60.1	60.1
obs refl	5355	43830	26443	21316
ind refl	4885	11959	12722	9693
refl used	4612	11953	12722	9693
R_{int}	0.034	0.051	0.057	0.039
R	0.073	0.062	0.095	0.076
R_w	0.103	0.063	0.125	0.109
GOF	1.82	0.97	1.01	1.01

[a] $C_4H_8O_2$ is ethyl acetate.

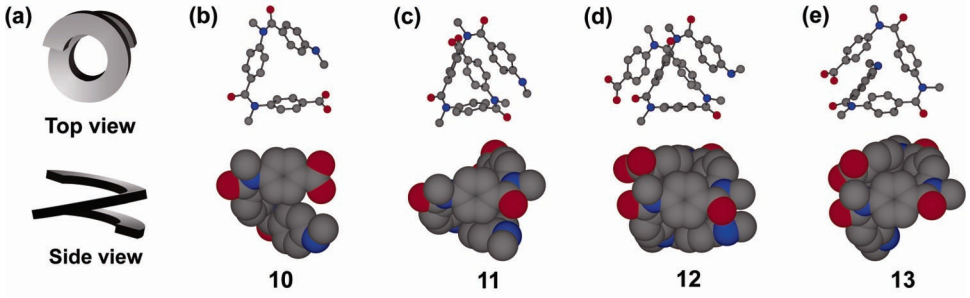

Figure 3. Top view (upper) and side view (lower) of (a) schematic representations and the crystal structures of (b) trimer **10**, (c) tetramer **11**, (d) pentamer **12**, and (e) *N*-Cbz and carboxylic acid-terminated tetramer **13**. Solvent molecules, terminal *O*-phenyl groups, and hydrogen atoms are omitted for clarity.

The crystal structure of **10** is shown in Figure 3b with schematic representations of the oligoamides in Figure 3a. The two amide bonds are in the cis conformation, and the terminal benzene rings are orientated at the same side of the plane of the central benzene ring (syn conformation), as expected. The top view of Figure 3b demonstrates that the three benzene rings are arranged in a cyclic manner. These structural properties are similar to those of *N*,*N*′-dimethylisophthalic dianilide.[12] Figure 3c,d shows the crystal structures of **11** and **12**, respectively. The structural properties of **11** and **12** are similar to those of **10**: all of the amide bonds are in the cis conformation, the consecutive three benzene rings are in the syn conformation, and the main chains are arranged in a cyclic manner (Figure 3c,d, top view). In addition, Figure 3 shows the growth of the helical motif from **10** to **11** and **12**: when one or two 4-(methylamino)benzoic acid units are added to the ester terminal of **10**, the additional units accumulate regularly on each unit of **10**. All of the properties mentioned previously clearly indicate that, in the crystal structures, **11** and **12** adopt a helical conformation with three monomer units per turn.

To investigate the effect of the terminal structure of the oligoamides on their conformation, the crystal structure of **13,** which has *N*-Cbz and carboxylic acid terminals, was determined by X-ray analysis (Figure 3e). A comparison of the structure of **13** with that of **11**, which has the same number of monomer units but different terminal structures, shows that the backbone arrangements are almost the same, and the conformation of **13** is also helical. The major difference between **11** and **13** lies in the tilt angles between the aromatic rings and the amide bonds.

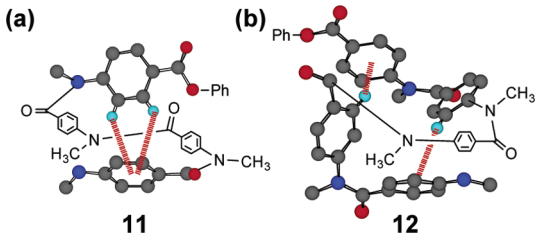

Figure 4. Intramolecular edge-to-face aromatic interactions (red dotted lines) in the crystal of (a) **11** and (b) **12**.

As shown in Figure 4, intramolecular edge-to-face aromatic interactions,[26] in which the ring center-hydrogen atom distance is between 3.07 and 3.45 Å, are observed in the crystal structures of **11** and **12**. However, we can find neither intramolecular aromatic interaction in **10** and **13** nor effective intermolecular interactions in **10**−**13**. These results indicate that the helical structures of **10**−**13** are enforced mainly by the inherent structural propensities of aromatic amide bonds, such as

(26) Jennings, W. B.; Farrell, B. M.; Malone, J. F. *Acc. Chem. Res.* **2001**, *34*, 885−894.

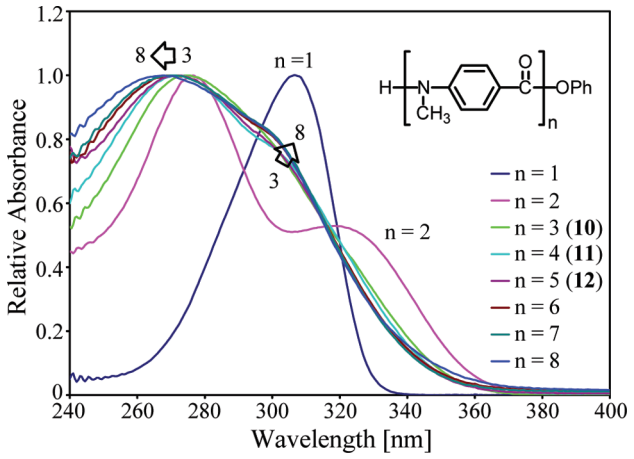

Figure 5. Room-temperature electronic absorption spectra of 4-(methylamino)benzoic acid oligomer phenyl esters in $CHCl_3$. The absorption intensity is normalized at the strongest peak. Concentration and observed absorbance at 300 nm: 1-mer (concentration = 7.6 mg/L, Abs_{300} = 0.93), 2-mer (34 mg/L, 0.98), 3-mer (20 mg/L, 0.97), 4-mer (22 mg/L, 0.89), 5-mer (23 mg/L, 0.96), 6-mer (17 mg/L, 0.89), 7-mer (20 mg/L, 0.86), and 8-mer (33 mg/L, 0.89).

regularity of C_{ortho}—C_{ipso}—N—C(=O) and C_{ortho}—C_{ipso}—C(=O)—N torsion angles, as well as the cis conformation of the amide bonds and the syn arrangement of the benzene rings. Considering the structural similarity of the polymers **1** and oligomers **10**−**13**, the conformation of *N*-alkylated poly(*p*-benzamide)s should be controlled by the same inherent factors, in accordance with the previously mentioned results that the polyamides **1** possess helical conformations independently of the solvent polarity.

4. UV Spectra of Oligo(benzamide)s. To reach a better understanding of the relations between the molecular structure and the spectral features, we measured electronic absorption spectra of a series of 4-(methylamino)benzoic acid oligomer phenyl esters up to an octamer (Figure 5). The single absorption band seen at ca. 300 nm for the monomer split into two distinct peaks (280 and 320 nm) in the dimer. These bands can be attributed to the transitions from the ground state to the higher and lower excited state as a result of the strong exciton interactions of the monomer units (details of the exciton analysis are discussed in section 5.2).[27] Interestingly, the spectral features of the other higher oligomers appeared to be similar to one another. The absorption peaks of these oligomers were observed in the range of 260−280 nm with a shoulder at ca. 300 nm, depending on the number of the repeating unit; as the number of chromophoric unit increased, the absorption peak of the oligomers blue-shifted systematically, while the shoulder band shifted to the red. More importantly, the absorption spectra of these oligomers were essentially identical to those of the polymers, implying that even small oligomers (trimer to octamer) are long enough to show a helical turn in solution.

5. Exciton CD Analysis. As mentioned in the second section, monomer **2** was almost CD silent, while polyamides **1** showed intense bisignate CD signals depending on temperature (0−45 °C), regardless of the solvent polarity. This experimental evidence substantiates that polymers **1** adopt a well-defined helical geometry under the experimental conditions. Since the crystal structures of the oligo(*N*-methyl-*p*-benzamide)s showed a partial turn of helix, the geometry of the polymers in solution can be deduced, as a first step, to be a helical conformation with three monomeric units per turn.

The key feature of the present system for analyzing spectra is that the polymer consists of a distinctive light-absorbing component, a 4-(alkylamino)benzoyl unit. This type of chromophore that has both electron-releasing and -withdrawing groups at para positions of benzene can be considered as a spectroscopically well-defined subunit that is only slightly perturbed by the rest of the system upon polymerization.[28] Thus, the electronic wave functions in the chromophore are assumed to have no electron exchange with the rest of the system. In such a case, Kasha's molecular exciton model has been applied to account for the electronic absorption and the CD spectral features of chiral oligomers and polymers.[27] The molecular exciton model is a state interaction perturbation theory that deals with the excited state resonance interaction among chromophores in weakly coupled electronic systems. Since the monomer unit considered here corresponds to an intrinsically achiral chromophore, the CD signals must be induced predominantly by the Kuhn−Kirkwood coupled-oscillator mechanism.[29] Nakanishi and Harada have successfully applied this theory to determine the absolute configurations of many natural organic molecules by measuring the CD spectra of their dibenzoate derivatives (dibenzoate exciton chirality method).[28]

5.1. TDDFT Calculations of a Model Monomer. Before applying the exciton theory to our system, we need to assign the absorption bands of the monomeric unit unambiguously so that the absorption spectrum of a model compound, 4-(methylamino)benzoic acid, was calculated using the time-dependent DFT method at the B3LYP/6-31G* level.[30] As shown in Figure 6, an intense absorption band was estimated to lie at 266 nm, reproducing well with the experimental absorption band of monomer **2** at ca. 300 nm (Figure 1). This band is associated predominantly with the HOMO → LUMO transition (ca. 89%) and polarized parallel to the long axis of the molecule. The two frontier orbitals indicate that the transition is of the $\pi-\pi^*$ type of a benzene chromophore with intramolecular CT character.[28] Thus, electrons rearrange from the electron-releasing amino side to the electron-withdrawing carbonyl side during the transition since the amino nitrogen and the carbonyl carbon contribute significantly to the benzene HOMO and LUMO levels, respectively. Essentially identical spectra were predicted by the semiempirical ZINDO/S calculations.[31] As a result, we can assume that the CD signals observed between 240 and 340 nm in the polymeric system (Figure 1) arise from excitonic interactions between the transitions along the long axis of each 4-aminobenzoyl chromophore.

5.2. Exciton Energy Level Diagram. To relate the spectroscopic properties observed in the benzamide system to their

(27) (a) Kasha, M.; Rawls, H. R.; El-Bayoumi, M. A. *Pure Appl. Chem.* **1965**, *11*, 371−392. (b) Kasha, M. In *Spectroscopy of the Excited State*; Bartolo, B., Eds.; Plenum: New York, 1976; pp 337−363.

(28) Harada, N.; Nakanishi, K. *Circular Dichroic Spectroscopy: Exciton Coupling in Organic Stereochemistry*; University Science Books: Mill Valley, CA, 1983.

(29) (a) Kuhn, W. *Trans. Faraday Soc.* **1930**, *26*, 293−308. (b) Kirkwood, J. G. *J. Chem. Phys.* **1937**, *5*, 479−491. (c) Tinoco, I. *Adv. Chem. Phys.* **1962**, *4*, 113−160. (d) Muranaka, A.; Okuda, M.; Kobayashi, N.; Somers, K.; Ceulemans, A. *J. Am. Chem. Soc.* **2004**, *126*, 4596−4604.

(30) (a) Furche, F.; Ahlrichs, R.; Wachsmann, C.; Weber, E.; Sobanski, A.; Vogtle, F.; Grimme, S. *J. Am. Chem. Soc.* **2000**, *122*, 1717−1724. (b) Dreuw, A.; Head-Gordon, M. *J. Am. Chem. Soc.* **2004**, *126*, 4007−4016. (c) Stephens, P. J.; McCann, D. M.; Devlin, F. J.; Cheeseman, J. R.; Frisch, M. J. *J. Am. Chem. Soc.* **2004**, *126*, 7514−7521.

(31) Ridley, J. E.; Zerner, M. C. *Theor. Chim. Acta* **1976**, *42*, 223−236.

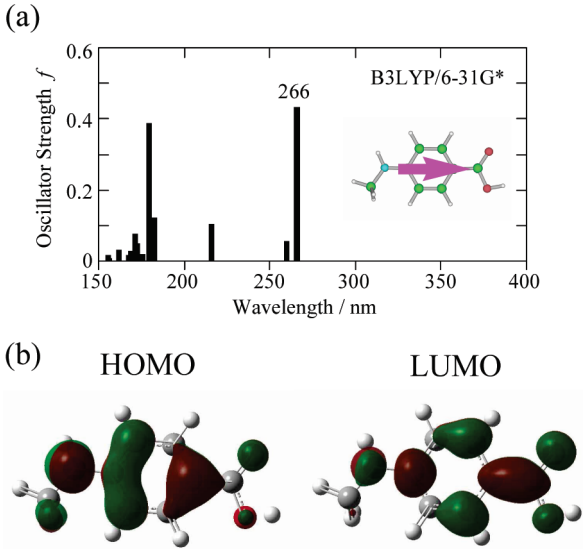

Figure 6. (a) Stick absorption spectrum of 4-(methylamino)benzoic acid as a model monomer calculated by the TDDFT method (B3LYP/6-31G* level). The arrow in the inset indicates the transition electric dipole moment ($\boldsymbol{\mu}$) corresponding to the lowest-energy transition. (b) Frontier molecular orbitals.

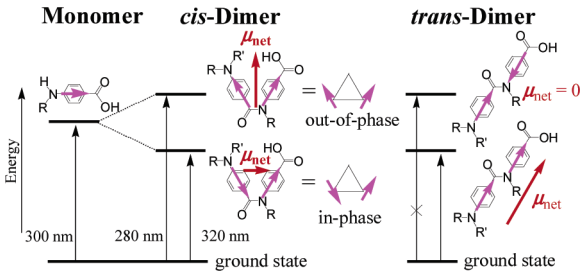

Figure 7. Schematic exciton band energy diagrams for *cis*- and *trans*-dimers of 4-(alkylamino)benzoic acid. The pink and red arrows indicate the transition electric dipole moments of each 4-(alkylamino)benzoyl chromophore and the net transition electric moments, respectively.

molecular geometry, first a qualitative exciton energy level diagram of the dimer is considered. Within the point−dipole approximation, the exciton interaction can be represented as a coupling of electric transition dipole moments ($\boldsymbol{\mu}$) of each chromophore.[27] Figure 7 shows the schematic energy diagram and the vector model for a *cis*-dimer whose conformation has been confirmed experimentally by the previous studies of *N*-methylbenzanilide.[11a] It is readily seen that the in-phase arrangement of the transition dipoles leads to an electrostatic attraction, producing a lower exciton state, whereas the out-of-phase arrangement of the transition dipoles causes repulsion, producing a higher exciton state. The magnitude of the net transition moment ($\boldsymbol{\mu}_{net}$) of the higher state is about 1.73 times larger than that of the lower state, so that the absorption intensity corresponding to a transition from the ground state to the higher exciton state becomes more intense than that to the lower exciton state, as is indeed observed in Figure 5. If the dimer adopts a trans conformation, the transition to the higher exciton state becomes optically forbidden because of the cancellation of the net moment. As a result, the experimental spectral data observed for the dimer are reasonably explained within the simple vector model for the *cis*-dimer.

We then consider a cyclic planar trimer as a model system for the helical polymer. As shown in Figure 8, the formation of a cyclic trimer results in three exciton states by its symmetry.[27]

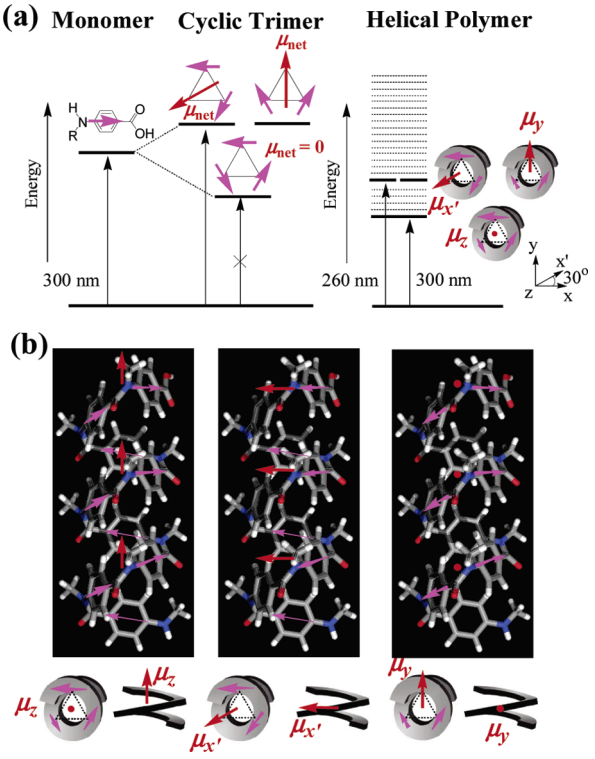

Figure 8. (a) Schematic exciton band energy diagrams for a cyclic trimer and a helical polymer with three light-absorbing units per turn. The pink and red arrows indicate the transition electric dipole moments of each 4-aminobenzoyl chromophore and the net transition electric moments, respectively. The dotted bands correspond to optically forbidden exciton bands for the polymer. (b) Optically allowed exciton states of the helical *N*-alkylated *p*-benzamide polymer. The geometry of the model oligomer was built using molecular mechanics calculations.

The lowest exciton state is optically forbidden due to a cancellation of the net transition dipole moment. The higher energy state, which has one nodal plane, is a doubly degenerate state with optically allowed nature. It is therefore possible to assign the absorption bands of the trimer in Figure 5. As would be expected, the low-energy exciton state in a helical trimer gains a net transition moment ($\boldsymbol{\mu}_z$) perpendicular to the plane since each transition moment in the trimer is not aligned in a plane in contrast to an ideal planar trimer. As a consequence, the absorption shoulder observed at around 300 nm can be attributed to the partially allowed transition to the lowest exciton state, the polarization of which is parallel to the helix axis. The absorption band with the center at ca. 260−270 nm should be a transition to the doubly degenerate higher-energy exciton state, which is polarized perpendicular to the helix axis.

The exciton band structure of a model helical polymer with three chromophoric units per turn is presented in the right-hand side of Figure 8a. In analogy with a cyclic trimer, the possible optical transitions by electric dipole radiation for larger polymers are severely limited by symmetry, although a quasi-continuous exciton band is generated.[27] In the present system, one of the optically allowed exciton states corresponds to the deepest exciton state, in which all electric transition moments couple one another, similar to the in-phase coupling of the *cis*-dimer and cyclic trimer. The other allowed state is doubly degenerate and has one nodal plane perpendicular to the helix axis, similar to the out-of-phase coupling of the dimer and trimer. Figure 8b shows each coupling mode corresponding to the optically allowed exciton states of the polymer. As a consequence, it is

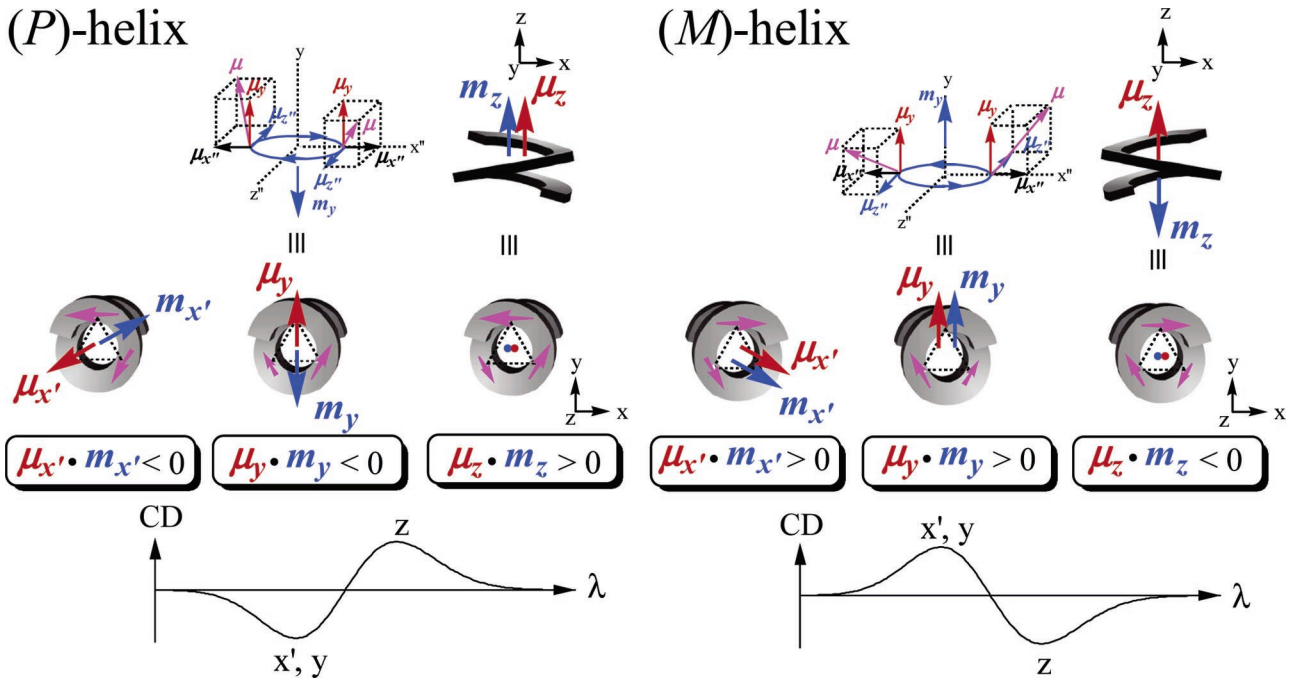

Figure 9. Overviews of the direction of the net electric (***μ***, red) and magnetic (***m***, blue) transition dipole moments. The theoretically predicted CD signals are shown at the bottom. Note that the *x*′′- and *z*′′-axes are tilted slightly as compared with the *x*- and *z*-axes. The blue circle represents a circulation of charge arising from the coupling of two transition electric moments.

possible to assign that the absorption shoulder and the positive CD band of poly(*N*-alkyl-*p*-benzamide)s **1** at ca. 300 nm arise from the transition to the lowest exciton state and that the intense absorption and the negative CD at ca. 260 nm are associated with the transition to the doubly degenerate exciton state.

5.3. Assignment of the Helical Structure of Polymer 1. To determine the helicity of the present polymeric system from the observed CD pattern, a qualitative coupled-oscillator analysis is performed.[29] In principle, the CD intensity (rotational strength *R*) of a transition in a collection of randomly oriented chiral molecules is expressed by the Rosenfeld equation;[32]

$$R = Im(\boldsymbol{\mu} \cdot \boldsymbol{m}) \qquad (1)$$

where ***μ*** is the transition electric dipole moment and ***m*** describes the transition magnetic dipole moment, which is related to the net circulation of electrons. The direction of ***m*** is such that when viewed from its tip, the rotation of charge is anticlockwise. *Im* denotes the imaginary part of ***μ***·***m***. The equation implies that the sign of the CD is simply determined by the relative arrangement of ***μ*** and ***m***. In the case of the present polymers, the two coupling modes that give rise to the lower energy positive CD and the higher energy negative CD bands were associated with the net electric transition moments that lie, respectively, parallel and perpendicular to the helix axis. Since the coupling between the transition electric moment (***μ***) and the magnetic moment (***m***) is described as a scalar product from the Rosenfeld equation, we need to consider only these transition moments along the same axis for determining the origin of the optical activity.

The overviews of the direction of the net transition moments for a right-handed ((*P*)-helix) and left-handed ((*M*)-helix) helical polymer with three light-absorbing units per turn are presented in Figure 9. It should be noted that the coupling of the transitions along the long axis induces the net transition magnetic dipole moment (***m***). The lower energy exciton state can be represented as head-to-tail couplings of neighboring transition moments, giving rise to a transition magnetic moment (***m***) parallel or antiparallel to the *z*-axis because of a circulation of the transition electric moments (***μ***). On the other hand, the doubly degenerate higher exciton state has a magnetic moment (***m***) directed along the *x*′- or *y*-axis. By considering the scalar product of ***μ*** and ***m***, a theoretical CD pattern can be predicted for our system. For example, in the case of the (*P*)-helix, ***m*** and ***μ*** become opposite in sign along the *x*′ and *y*-axes, which generate CD at shorter wavelengths so that the CD sign becomes negative, while they are the same sign along the *z*-axis so that a positive CD signal is observed at longer wavelengths. Note that the positive and negative CD signals have the same intensity because of the sum rule.[28] As would be expected, the CD pattern of the (*M*)-helix is the mirror image of that of the (*P*)-helix. Since the CD patterns of polymer **1** we studied exhibited a plus-to-minus CD pattern, in ascending energy, with the almost identical intensity, it can be concluded that *N*-alkylated poly(*p*-benzamide) **1** preferentially takes a right-handed helical geometry ((*P*)-helix) in chloroform, methanol, and acetonitrile. TDDFT (B3LYP/6-31G*) calculations of the crystal structures of the oligo(*N*-methyl-*p*-benzamide) phenyl esters support this assignment, although the number of the monomer units, the crystal packing, and the terminal phenyl groups may contribute to the CD spectra to some extent (see Supporting Information). Hence, the calculated CD spectrum of the (*P*)-trimer shows a plus-to-minus CD pattern, while that of (*M*)-tetramer shows a minus-to-plus CD pattern, in agreement with the assignment based on the molecular exciton model.

(32) Rodger, A.; Nordén, B. *Circular Dichroism and Linear Dichroism*; Oxford University Press: Oxford, 1997.

Conclusion

In conclusion, we have demonstrated that the polyamides **1**, synthesized by chain-growth polycondensation of **2**, take a helical structure in solution, based upon the following: (1) significant amplification of the CD signal of the polymer as compared with that of the monomer, (2) temperature dependence of the CD signal, with the higher values at lower temperature, and (3) chain length (or molecular weight) dependence of the CD spectra. The helical structure in the solid state was also confirmed by X-ray crystallographic analysis of the *N*-methyl aromatic oligoamides **10**−**13**, which show a helical conformation with three monomer units per turn, despite their highly flexible backbone. The helical structure of *N*-alkylated poly(*p*-benzamide)s probably stems from the inherent structural propensities of cis conformation of *N*-alkylated amide bonds and syn arrangement of the benzene rings.

It has been further demonstrated that the present exciton model analysis provides a clear-cut picture for qualitative understanding of the secondary structure of *N*-alkylated poly(benzamide)s in solution. The positive and negative CD signals observed at 300 and 260 nm, respectively, in the polymeric system were successfully assigned to the exciton bands arising from the couplings of the long axis polarized transition of each 4-(alkylamino)benzoyl chromophore. Taking into account the Rosenfeld equation, we have elucidated that polymer **1** preferentially adopts a right-handed helical structure ((*P*)-helix) under the experimental conditions. It is important to note that the helicity of the polymer could be derived, without a great deal of calculation, by inspection of the CD spectra and applying the molecular exciton model, despite its crude nature.

Experimental Procedures

Syntheses of **10**−**13** are described in the Supporting Information. Column chromatography was performed on a silica gel (Silica gel 60, spherical, 40−100 μm, Kanto or Kieselgel 60, 230−400 mesh, Merck) with a specified solvent. Commercially available (Kanto) tetrahydrofuran (THF, stabilizer-free) was used as a dry solvent. ^{1}H NMR spectra were obtained on an ECA-600 spectrometer with tetramethylsilane as the internal standard (0.00 ppm). Mass spectra were recorded on a JEOL JMA-HX110 spectrometer. The M_n and M_w/M_n values of polymers were measured on a Shodex GPC-101 equipped with Shodex UV-41, Shodex RI-71S, and DAWN EOS multiangle laser light scattering (MALLS, Wyatt Technology Corp) detectors and two Shodex KF-804L columns (bead size = 7 μm, pore size = 200 Å). THF was used as the eluent (temperature = 40 °C, flow rate = 2 mL/min). Calibration was carried out using polystyrene standards. Isolation of polyamides was carried out with a Japan Analytical Industry LC-908 Recycling Preparative HPLC (eluent: chloroform) with the use of two TOSOH TSK-gel columns (2× G2000H$_{HR}$). UV−vis spectra were measured on a JASCO V-550 spectrometer. CD spectra were measured on a JASCO J-820 using a 10 mm quartz cell. The concentration of each solution for CD and UV experiments was adjusted so that the absorbance at 300 nm was 1.

Synthesis of 4. 2-Nitrobenzenesulfonyl chloride (0.239 g, 1.1 mmol, 1.1 equiv) was added to a solution of **3**[14h] (0.205 g, 0.96 mmol) in pyridine (1 mL) at 0 °C. The reaction mixture was stirred at room temperature for 2 h and poured into 1 M hydrochloric acid (20 mL). The aqueous layer was extracted with CH_2Cl_2 twice. The combined organic extracts were washed with brine, dried over anhydrous Na_2SO_4, and evaporated. The residue was purified by silica gel column chromatography (AcOEt/hexane = 1/3) to give **4** as a white solid (0.367 g, 96%). ^{1}H NMR (600 MHz, $CDCl_3$) δ 8.13 (d, J = 8.6 Hz, 2 H), 7.98 (d, J = 7.9 Hz, 1 H), 7.89 (d, J = 7.9 Hz, 1 H), 7.74 (t, J = 7.9 Hz, 1 H), 7.65 (t, J = 7.9 Hz, 1 H), 7.50 (s, 1 H), 7.42 (t, J = 7.0 Hz, 2 H), 7.37 (d, J = 6.9 Hz, 2 H), 7.27 (t, J = 7.0 Hz, 1 H), 7.17 (d, J = 8.6 Hz, 2 H).

Synthesis of 6. Diethyl azodicarboxylate (DEAD, 40% in toluene, 5.75 g, 13 mmol) was added to a solution of **4** (4.78 g, 12 mmol), **5**[20] (1.50 g, 8.1 mmol), and PPh_3 (3.47 g, 13 mmol) in dry THF (40 mL) at 0 °C under an Ar atmosphere. The reaction mixture was stirred at room temperature for 15 h and evaporated. The residue was purified by silica gel column chromatography (AcOEt/hexane = 1:1) to give **6** as a colorless oil (3.16 g, 67%). ^{1}H NMR (600 MHz, $CDCl_3$) δ 8.14 (d, J = 8.6 Hz, 2 H), 7.66 (t, J = 7.9 Hz, 1 H), 7.62 (d, J = 7.9 Hz, 1 H), 7.59 (d, J = 7.9 Hz, 1 H), 7.50 (t, J = 7.9 Hz, 1 H), 7.47 (d, J = 8.6 Hz, 2 H), 7.44 (t, J = 7.6 Hz, 2 H), 7.29 (t, J = 7.6 Hz, 1 H), 7.20 (d, J = 7.6 Hz, 2 H), 3.93−3.87 (m, 2 H), 3.64−3.58 (m, 4 H), 3.53−3.49 (m, 4 H), 3.46−3.42 (m, 1 H), 3.37 (s, 3 H), 1.21 (d, J = 6.5 Hz, 3 H).

Synthesis of 2. A solution of benzenethiol (0.754 g, 6.8 mmol) in CH_3CN (20 mL) and Cs_2CO_3 (5.62 g, 17 mmol) was added to a solution of **6** (3.16 g, 5.7 mmol) in CH_3CN (60 mL). The reaction mixture was heated at 70 °C for 2 h and allowed to cool to room temperature. The reaction mixture was diluted with water and extracted with CH_2Cl_2. The organic layer was washed with brine, dried over anhydrous Na_2SO_4, and evaporated. The residue was purified by silica gel column chromatography (AcOEt/hexane = 1:1) to give **2** as a yellow oil (1.88 g, 89%). ^{1}H NMR (600 MHz, $CDCl_3$) δ 8.01 (d, J = 8.6 Hz, 2 H), 7.40 (t, J = 7.6 Hz, 2 H), 7.23 (t, J = 7.6 Hz, 1 H), 7.19 (d, J = 7.6 Hz, 2 H), 6.63 (d, J = 8.6 Hz, 2 H), 5.01 (br s, 1 H), 3.81−3.75 (m, 2 H), 3.69−3.66 (m, 4 H), 3.61−3.58 (m, 3 H), 3.40 (s, 3 H), 3.33−3.29 (m, 1 H), 3.14−3.10 (m, 1 H), 1.25 (d, J = 6.2 Hz, 3 H). HRFAB-MS [M + H] Calcd for $C_{21}H_{28}NO_5$: 374.1967; Found: 374.1969.

Typical Procedure of Polymerization: Synthesis of Polyamide 1f. CsF (0.083 g, 0.55 mmol) was placed in a round-bottomed flask and dried by being heated at 250 °C under reduced pressure for 20 min. A solution of **7** (0.0024 g, 0.0099 mmol), **2** (0.185 g, 0.49 mmol), and *N*-octyl-*N*-triethylsilylaniline (0.151 g, 0.47 mmol) in 0.7 mL of dry THF was added to the flask under a N_2 atmosphere. A solution of 18-crown-6 (0.272 g, 1.03 mmol) in 0.3 mL of dry THF was added to the mixture at room temperature, and the whole was stirred overnight at room temperature. The reaction mixture was quenched with saturated aqueous ammonium chloride (4 mL) and extracted with CH_2Cl_2. The organic layer was washed with water, dried over anhydrous Na_2SO_4, and evaporated. Removal of *N*-octylaniline and isolation of the polymer formed were carried out by preparative HPLC (eluent: chloroform) with the use of polystyrene gel columns to afford the polyamide **1f** (0.0825 g).

X-ray Crystallography. The structural determination of compound **10** was made on a Rigaku AFC5R diffractometer with graphite-monochromated Cu Kα radiation at 296 K to a maximum 2θ value of 145.3°. The structure was solved by direct methods (SIR92) and expanded using Fourier techniques (DIRDIF94). The non-hydrogen atoms were refined anisotropically. The structural determinations of compounds **11**−**13** were made on a Rigaku RAXIS-RAPID Imaging Plate diffractometer with graphite-monochromated Mo Kα radiation

(33) Frisch, M. J.; Trucks, G. W.; Schlegel, H. B.; Scuseria, G. E.; Robb, M. A.; Cheeseman, J. R.; Montgomery, J. A., Jr.; Vreven, T.; Kudin, K. N.; Burant, J. C.; Millam, J. M.; Iyengar, S. S.; Tomasi, J.; Barone, V.; Mennucci, B.; Cossi, M.; Scalmani, G.; Rega, N.; Petersson, G. A.; Nakatsuji, H.; Hada, M.; Ehara, M.; Toyota, K.; Fukuda, R.; Hasegawa, J.; Ishida, M.; Nakajima, T.; Honda, Y.; Kitao, O.; Nakai, H.; Klene, M.; Li, X.; Knox, J. E.; Hratchian, H. P.; Cross, J. B.; Adamo, C.; Jaramillo, J.; Gomperts, R.; Stratmann, R. E.; Yazyev, O.; Austin, A. J.; Cammi, R.; Pomelli, C.; Ochterski, J. W.; Ayala, P. Y.; Morokuma, K.; Voth, G. A.; Salvador, P.; Dannenberg, J. J.; Zakrzewski, V. G.; Dapprich, S.; Daniels, A. D.; Strain, M. C.; Farkas, O.; Malick, D. K.; Rabuck, A. D.; Raghavachari, K.; Foresman, J. B.; Ortiz, J. V.; Cui, Q.; Baboul, A. G.; Clifford, S.; Cioslowski, J.; Stefanov, B. B.; Liu, G.; Liashenko, A.; Piskorz, P.; Komaromi, I.; Martin, R. L.; Fox, D. J.; Keith, T.; Al-Laham, M. A.; Peng, C. Y.; Nanayakkara, A.; Challacombe, M.; Gill, P. M. W.; Johnson, B.; Chen, W.; Wong, M. W.; Gonzalez, C.; Pople, J. A. *Gaussian 03*, Rev. B.04; Gaussian, Inc.: Pittsburgh, PA, 2003.

at 93 K for **11** and **13** or 113 K for **12** to a maximum 2θ value of 60.1°. The structures were solved by direct methods (SIR97) and expanded using Fourier techniques (DIRDIF94). The non-hydrogen atoms were refined anisotropically.

Calculation. All calculations were carried with a Gaussian 03 (G03) program package[33] using the hybrid density functional method based on Becke's three-parameter exchange function and the Lee−Yang−Parr nonlocal correlation functional (B3LYP).[34] We used 6-31G* basis set for all atoms. Geometry optimization and time-dependent DFT calculations were performed at the same level.

Acknowledgment. We thank Yuko Inagaki for the UV measurements. This work was partially supported by a Grant-in-Aid (15750108 and 17350063) for Scientific Research and the COE project, Giant Molecules and Complex Systems, 2005, from the Ministry of Education, Culture, Sports, Science and Technology, Japan.

(34) (a) Becke, A. D. *Phys. Rev.* **1988**, *A38*, 3098−3100. (b) Becke, A. D. *J. Chem. Phys.* **1993**, *98*, 1372−1377. (c) Becke, A. D. *J. Chem. Phys.* **1993**, *98*, 5648−5652. (d) Lee, C.; Yang, W.; Parr, R. G. *Phys. Rev.* **1988**, *B37*, 785−788.

Supporting Information Available: Synthesis of **8**−**13** and other phenyl esters of 4-(methylamino)benzoic acid oligomers, M_n and M_w/M_n of **8**, correlation plot of the values of M_n of **1** determined by ^{1}H NMR to those determined by GPC and MALLS, UV and CD spectra measured in methanol, dependence of CD intensities on molecular weight of polyamide **1f** measured in CH_3CN and CH_3OH at various temperatures, crystallographic information (ORTEP drawings and CIF files) of oligoamides **10**−**13**, and calculated UV and CD spectra of the phenyl esters of the oligo(*N*-methyl-*p*-benzamide). This material is available free of charge via the Internet at http://pubs.acs.org.

JA0455291